IEEE Access
Multidisciplinary | Rapid Review | Open Access Journal

Received August 3, 2018, accepted September 4, 2018, date of publication September 10, 2018, date of current version October 8, 2018.

Digital Object Identifier 10.1109/ACCESS.2018.2869402

Constrained Multiple Model Particle Filtering for Bearings-Only Maneuvering Target Tracking

HONGWEI ZHANG, LIANGQUN LI, AND WEIXIN XIE
ATR Key Laboratory, Shenzhen University, Shenzhen 518060, China

Corresponding author: Liangqun Li (lqli@szu.edu.cn)

This work was supported in part by the National Natural Science Foundation of China under Grant 61773267 and in part by the Science and Technology Program of Shenzhen under Grant JCYJ20170302145519524 and Grant JCYJ20170818102503604.

ABSTRACT This paper presents an effective constrained multiple model particle filtering (CMMPF) for bearings-only maneuvering target tracking. In the proposed algorithm, the process of target tracking is factorized into two sub-problems: 1) motion model estimation and model-conditioned state filtering according to the Rao–Blackwellised theorem and 2) the target dynamic system is modeled by multiple switching dynamic models in a jump Markov system framework. To estimate the model set, a modified sequential importance resampling method is used to draw the model particles, which can be restricted into the feasible area coincide with the constrained bound. To the model-conditioned state nonlinear filtering, a truncated prior probability density function is constructed by utilizing the latest observations and auxiliary variables (target spatio–temporal features), which can guarantee the diversity and accuracy of the sampled particles. The tracking performance is compared and analyzed with other conventional filters in two scenarios: 1) uniform and time-invariant sampling scenario and 2) non-uniform and sparse sampling scenario. A conservative Cramer–Rao lower bound is also introduced and compared with the root mean square error performance of the suboptimal filters. Simulation results confirm the superiority of CMMPF algorithm over the other existing ones in comparison with respect to accuracy, efficiency, and robustness for the bearings-only target tracking system, especially for the aperiodic and sparse sampling environment.

INDEX TERMS Bearings-only maneuvering target tracking, constrained bound, constrained multiple model particle filtering, Cramer-Rao lower bound.

I. INTRODUCTION

Bearings-only tracking uses only the noise-corrupted angular data to estimate the current state parameters (ie., positon and velocity) [1]–[3]. In recent decades, this method has been widely used in a variety of important practical applications, such as radar, aerospace and computer vision. Due to inherent nonlinearity and observability issues, it is difficult to construct a finite-dimensional optimal Bayesian filter, as for the bearings-only tracking of a maneuvering target, the problem is much more difficult and so far, very limited research has been published in the open literature. The multiple model adaptive estimate (MMAE) [4], [5] approach runs a set of parallel single-model-based filters, which are independent of each other. This approach works well with an unknown structure or parameters but requires no structural or parametric changes. One common approach to overcome this difficulty is the interacting multiple-model (IMM)-based estimator [6]–[8], the models obey a Markov sequence, switching from one model to another in a probabilistic manner. For IMM-based trackers, model design should consider both the quality and complexity of the model. Typically, the models used in the air traffic control tracking will include one for the uniform motion and one or more for the maneuver. [6]. Accurate motion modeling and nonlinear filtering are two challenging problems that should not be separated. Taylor-series expansion (TSE) is a fundamental tool for handling nonlinearity. The first-order extended Kalman filter (EKF), which has been no doubt the most widely used to in nonlinear filtering algorithm for state estimation, including target tracking for its simplicity and generality. But the EKF is adequate only when the noise is sufficiently small, which can rarely be guaranteed [9], [10]. The unscented Kalman filter (UKF) algorithm selects a few Gaussian points to approximate a nonlinear distribution, raising the accuracy to third order, leading to more accurate results and much better estimates of the covariance of the states than the EKF. Nevertheless, these

KF-type filters, have the limitation that the filtering method does not apply to general non-Gaussian distributions [10], [11]. Another popular solution strategy for the general nonlinear filtering problem is the sequential Monte Carlo (SMC) methods, also known as particle filters (PFs) [12], [13], which allow for a complete representation of the posterior distribution of the estimated states in an online manner, in principle, the approach can deal with any nonlinear and non-Gaussian estimation problems by drawing an infinite number of particles theoretically. But the computation complexity is expensive especially for high dimension. One method of improving the efficiency and reducing the coariance of SMC is to utilizing Rao-Blackwellised approach [13], [14], which computes the conditionally Gaussian component in a closed form and is always more accurate than any finite set and has less variance than pure Monte Carlo sampling. Based on the Rao-Blackwellised structure, Liu *et al.* [15] investigated the formulation of the correlation between the two linear and nonlinear components, solved the deviation problem by correctly updating the conditioned linear model estimation with the information from the nonlinear state filtering, and finally reduced the estimation error in maneuvering target tracking.

In actual applications, the stochastic nonlinearity of a stochastic dynamic system is always limited by the subregions of the state space in the presence of state constraints. Truncated methods can often effectively improve the tracking performance in nonlinear filtering. In [16], a truncated unscented Kalman filter were proposed, improving the accuracy of posterior density in the region of interest. Meanwhile the state vector distribution becomes highly non-Gaussian due to truncated edge probability density function (PDF), and thus, the KF-type filters are not applicable. While the constrained particle filters show merits for this problem [17]. Li *et al.* [18] proposed an auxiliary truncated particle filter by modifying the priori PDF, which handles the abrupt target maneuvering more effectively compared with the corresponding Monte Carlo simulation without constraints when dealing with the bearing-only target maneuvering tracking. Xu *et al.* [19] incorporated the nonlinear state constraints into the dynamic model establishment, deduced the revised state prediction and updating process to realize the optimization control which satisfies certain variance criterion. Heng *et al.* [20] proposed to design a more efficient SMC method using an optimal control which can achieve the same accuracy with fewer particles, deduced the correlation between iterative recursion and optimal control strategy and aimed to extend the existing particle filtering method to the static model.

In this paper, the angular measurements are collected by two passive sensors on two stationary platforms which are assumed to be connected by a tactical data link capable of transmitting measurements as they occur synchronously with a zero transmission delay. Furthermore, it is assumed that the probability of target detection is unity and there are no false alarms (thus ignoring the data association issues). The proposed CMMPF-based estimator divided the maneuvering target tracking process into two components: motion model estimation and model-conditioned state nonlinear filtering. Based on the assumption that this approach can probabilistically draw model particles with a higher likelihood of output measurement, a series of optimizations are enforced to work out the proposal distribution with the measurement constraints knowledge. For the state nonlinear filtering, the approach simultaneously introduces the latest measurement and target spatio-temporal features into the modified prior PDF by an efficient LS method, the prior density is jointed adaptively to enhance the estimate accuracy.

The tracking performance of CMMPF is compared with other conventional filters, they are two IMM-based estimator schemes, IMMEKF and IMMUKF, which uses EKF and UKF to compute the model-conditioned state estimation, respectively; JMS-PF which factorizes estimation into the model sequence given measurements and state estimation using a standard EKF method [7]; multiple model Rao-Blackllised particle filter (MMPF), and auxiliary truncated particle filter (ATPF) [18]. The Monte Carlo (MC) simulations are carried out in two scenarios: (i) Uniform and time-invariant sampling scenario and (ii) Non-uniform and sparse sampling scenario. The filtering performance is analyzed and compared to the ideal estimate Cramer-Rao lower bound (CRLB) [5], [7].

The remainder of the paper is organized as follows. Mathematical formulations for the bearings-only target maneuvering tracking problem and basic theory of CMMPF algorithm are introduced in Section II. Design and discussion of the proposed CMMPF algorithm are described in Section III. Whereas simulations and analysis of all algorithms in comparison are illustrated in Section IV. Finally, some concluded conclusions are presented in Section V.

II. STOCHASTIC DYNAMIC SYSTEM AND BASIC THEORY

A. STOCHASTIC DYNAMIC SYSTEM

The basic problem in bearings-only maneuvering target tracking is to estimate the trajectory of a target (i.e., position and velocity) from noise corrupted bearings data. In this paper we assume the target motion is modelled by multiple switching regimes, also known as jump Markov system (JMS) [21]. This means that the usual target state vector $\mathbf{x}_k = [x_1, \cdots, x_n] \in \Re^{n_x}$ is appended with a discrete model (or regime) variable $M \in \{M_1, \cdots, M_K\}$, where K is the number of possible models, whose transitions are modelled with a Markov chain. And then a three-dimensional(3D) model-conditioned target state vector is denoted as

$$\mathbf{x}_{m,k} = (x_{m,k}, \dot{x}_{m,k}, y_{m,k}, \dot{y}_{m,k}, z_{m,k}, \dot{z}_{m,k})^T \tag{1}$$

where subscript index k is the discrete time step, $(x_{m,k}, y_{m,k}, z_{m,k})$ and $(\dot{x}_{m,k}, \dot{y}_{m,k}, \dot{z}_{m,k})$ denote the motion-conditioned position and velocity components, respectively. A class of stochastic hybrid systems with additive noise can be can be mathematically written as

$$x_k = f_k(x_k, M_k) + g_k(x_k, M_k)v_k \tag{2}$$
$$z_k = h_k(x_k) + e_k \tag{3}$$

where $x_k \in \Re^{n_x}$ is the state vector at time k; v_k and e_k are the process and measurement noise vector, respectively; $z_k = [z_1, \cdots, z_n] \in \Re^{n_z}$ is the measurement sequence at time k. $f(\cdot)$, $g(\cdot)$ and $h(\cdot)$ are in general nonlinear vector-valued functions depending on the problem considered.

A typical target maneuver, such as a turn, often has an approximately constant speed and turn rate, most 2D and 3D target maneuver models are naturally turn motion models which are usually established relying on target kinematics [4]. For the JMS framework considered in this paper, the target motion obeys one of three dynamics behavior models: (a) standard constant velocity (CV) model, while the other two correspond to coordinated turn (CT) models that capture the maneuver dynamics. (b) clockwise CT model, and (c) anticlockwise CT model. Let $M_k \in \{1, 2, 3\}$ denote the model set, whose evolution follows a first order Markov chain. For the first CV model, the dynamic formula can be written as

$$\mathbf{x}_k = \begin{bmatrix} 1 & T & 0 & 0 & 0 & 0 \\ 0 & 1 & 0 & 0 & 0 & 0 \\ 0 & 0 & 1 & T & 0 & 0 \\ 0 & 0 & 0 & 1 & 0 & 0 \\ 0 & 0 & 0 & 0 & 1 & T \\ 0 & 0 & 0 & 0 & 0 & 1 \end{bmatrix} \mathbf{x}_{k-1} + \begin{bmatrix} T^2/2 & 0 & 0 \\ T & 0 & 0 \\ 0 & T^2/2 & 0 \\ 0 & T & 0 \\ 0 & 0 & T^2/2 \\ 0 & 0 & T \end{bmatrix} \mathbf{v}_k \tag{4}$$

with the CV model transition matrix is

$$F^{(1)}(x_k) = \begin{bmatrix} 1 & T & 0 & 0 & 0 & 0 \\ 0 & 1 & 0 & 0 & 0 & 0 \\ 0 & 0 & 1 & T & 0 & 0 \\ 0 & 0 & 0 & 1 & 0 & 0 \\ 0 & 0 & 0 & 0 & 1 & T \\ 0 & 0 & 0 & 0 & 0 & 1 \end{bmatrix} \tag{5}$$

where T denotes the sampling time, and $\mathbf{v}_k$ is a 3x1 i.i.d. process noise vector with $\mathbf{v}_k \sim N(0, Q)$. The process noise covariance matrix is chosen to be $Q = \sigma_k^2 I$, where I is the 3x3 identity matrix and σ_k is the standard deviation (STD) for process noise. The next two transition matrices correspond to constant turn (CT) transitions (clockwise and anticlockwise, respectively). These are given by

$$F^{(j)}(x_k) = \begin{bmatrix} 1 & \frac{\sin(T \cdot w)}{w} & 0 & -\frac{1-\cos(T \cdot w)}{w} & 0 & 0 \\ 0 & \cos(T \cdot w) & 0 & -\sin(T \cdot w) & 0 & 0 \\ 0 & \frac{1-\cos(T \cdot w)}{w} & 1 & \frac{\sin(T \cdot w)}{w} & 0 & 0 \\ 0 & \sin(T \cdot w) & 0 & \cos(T \cdot w) & 0 & 0 \\ 0 & 0 & 0 & 0 & 1 & T \\ 0 & 0 & 0 & 0 & 0 & 1 \end{bmatrix} \quad j = 2, 3 \tag{6}$$

where w is a constant angular turn rate; $w > 0$ describes a clockwise turn for CT correct model 2, and $w < 0$ for anti-clockwise CT opposite model 3. The process noise covariance matrix Q^2 is the same as that in CV model 1.

The target dynamic model jump (switch) process is modelled as a homogeneous Markov chain with known and time-invariant probabilities as

$$p_{ij} = P\left\{M_k = m_j | M_{k-1} = m_i\right\} \tag{7}$$

which are independent of the target state. The initial model probabilities $\pi_i = \{M_0 = m_i\}$ are also known.

In this paper, the angular measurements are collected by two passive sensors on the stationary platforms, denoted as $z_k^j = [z_{1,k}^j, \cdots, z_{n,k}^j] \in \Re^{n_z}$ where the subscript k denotes the time when the measurement was recorded and superscript $j \in \{1, 2\}$ denotes the *jth* observer (sensor) which supplies the measurements. The nonlinear measurement formula [1] can be rewritten as

$$\begin{aligned} & h_j(\mathbf{x}_{j,k}) \\ &= \begin{pmatrix} \theta_{j,k} \\ \beta_{j,k} \end{pmatrix} \\ &= \begin{pmatrix} \arctan\left(\dfrac{y_{j,k} - y_{s_j}}{x_{j,k} - x_{s_j}}\right) \\ \arctan\left(\dfrac{z_{j,k} - z_{s_j}}{\sqrt{\left(x_{j,k} - x_{s_j}\right)^2 + \left(y_{j,k} - y_{s_j}\right)^2}}\right) \end{pmatrix} \quad j = 1, 2 \end{aligned} \tag{8}$$

where $\mathbf{x}_{j,k} = (x_{j,k}, y_{j,k}, z_{j,k})$ define the target location in the 3D space from the *jth* sensor at time k; $\theta_{j,k}$ and $\beta_{j,k}$ denotes the azimuth and elevation angles of aircraft at time k, respectively, which are measured by the *jth* sensor and transmitted to the fusion node; $\mathbf{x}_{s_j} = (x_{s_j}, y_{s_j}, z_{s_j})$ is the location of the *jth* sensor; e_{s_j} denotes the measurement noise in *jth* sensor, which is assumed to be zero-mean white Gaussian with variance $R_{s_j} = \begin{bmatrix} 1 & 0 \\ 0 & 1 \end{bmatrix} \sigma_{s_j}^2$, independent of measurement noise in the other sensor and the process noise $\mathbf{v}_k$. Due to the band-width constraints, however, not all of the messages are transmitted, so that the tracking filter on *jth* platform receives all the local measurements and only occasional external messages via the data link. Time delays in the transmission are assumed to be zero.

B. BASIC THEORY OF CMMPF

In practice, it should be noted that the measurement noise is always boundary because no noise can supply an infinitely large value and thus the truncation theorem can be used in constrained optimization. To simplify the algorithm derivation, the target state vector is represented as $x_k = [a_k^T, b_k^T]^T$, where $a_k \in R^{n_a}$ and $b_k \in R^{n_b}$ denote the position and velocity vectors of the target state, respectively, $n_x = n_a + n_b$.

Such that, the equation (2) can be rewritten as

$$z_k = h_k(a_k) + e_k \tag{9}$$

where $h(\cdot)$ is the nonlinear function of a_k. The derivation should be subject to two basic hypotheses: 1), the measurement function $h(\cdot)$ in (3) is a bijective, continuous function; 2), the density of the additive measurement noise e_k, $p_{e_k}(e_k)$ has a bounded, connected support, i.e.,

$$p_{e_k}(e_k) = 0, e_k \notin I_{e_k} \subset R^{n_z} \tag{10}$$

where I_{e_k} is an n_z dimensional connected region.

According to the hypotheses 2), the measurement likelihood function given the state can be written as a truncated PDF as

$$\begin{aligned} p(z_k|x_k) &= p(z_k|a_k) \\ &= p_{ek}(z_k - h(a_k))\chi_{I_{ek}(z_k)}(z_k - h(a_k)) \end{aligned} \tag{11}$$

where $\chi_{I_{ek}(z_k)}$ is the indicator function on the sub-region $I_{ek}(z_k)$, which can be defined as

$$\chi_{I_{ek}(z_k)}(x_k) = \begin{cases} 0, & e_k \notin I_{ek} \subset R^{n_z} \\ 1, & e_k \in I_{ek} \subset R^{n_z} \end{cases} \tag{12}$$

Let $\wp_k$ denote the feasible area of state $x_{m,k}$ that satisfies the constraints condition

$$\wp_k = \left\{x_{m,k}|e_k \in I_{e_k} \subset R^{n_z}\right\} = \left\{a_{m,k}|e_k \in I_{e_k} \subset R^{n_z}\right\} \tag{13}$$

Applying Bayes' rule and the Rao-Blackwellised theorem, the full posterior distribution $p(x_{m,k}|z_k)$ at time k can be factorized as

$$\begin{aligned} &p(x_{m,k}|x_{1:k-1}, M_{1:k-1}, z_{1:k}) \\ &\quad = p(x_{m,k}|x_{1:k-1}, M_k, z_{1:k})p(M_k|x_{1:k-1}, M_{1:k-1}, z_{1:k}) \\ &\qquad s.t.\ \left\{x_{m,k}\right\} \in \wp_k \end{aligned} \tag{14}$$

In doing so, the drawn motion model particles can be restricted in a feasible area that satisfies the constraint conditions. Meanwhile, the covariance of the joint estimator can be calculated as

$$\mathrm{Var}\left[\eta(x, M)\right] = \mathrm{Var}\left[E(\eta(x, M)|x)\right] + \mathrm{Var}\left[E(\eta(x, M)|M)\right] \tag{15}$$

Because $\mathrm{var}E(\eta(x, M)|x)$ is non-negative, the covariance of the estimator $h' = E(h(x, M)|M)$ is less than the covariance of $\eta(x, M)$, it is clear that the suboptimal estimation reduces the estimation error.

The specific evolution and detailed derivation of the proposed CMMPF algorithm will be described in Section III.

III. DESIGN OF CMMPF

Taking advantage of both measurement constraints and auxiliary variables could yield more accurate estimate. In this regard, we develop a new CMMPF algorithm for bearings-only maneuvering target tracking. The design of CMMPF algorithm will be described in this section. The model-set estimation is presented in Section A, model-conditioned state estimation is represented in Section B, the summary and discussion of the CMMPF are given in Section C.

A. MODEL-SET ESTIMATE

At first, we now derive the model-set measurement likelihood function in presence of state constraints. The target motion model set $M_k \in \{1, 2, 3\}$ are assumed to be independent of each other. If the measurement z_{kj} is related to the target motion model m, the measurement likelihood can be given by

$$\begin{aligned} &p_{lik}(z_{kj}|M_k = m, z_{1:k-1}, M^i_{k-1}) \\ &= \int p(z_{kj}|M_k = m, x_{m,k})p(x_{m,k}|z_{1:k-1}, M^i_{k-1})dx_{m,k} \\ &= \int N(z_{kj}|h(x_k, M_k = m), R)N(x_{m,k}|f(x_{k-1}, M^i_{k-1}), Q)dx_{m,k} \end{aligned} \tag{16}$$

where j denotes the jth observer.

Such that, the measurement likelihood function can be derived by (2) and (16) as

$$\begin{aligned} &P_{lik}(z_k|M^i_k = m.z_{1:k-1}.M^i_{k-1}, r_{1:k}) \\ &= N(z_{kj}|h(f(x_{k-1}, M^i_{k-1}), M_k = m, r_k), S_{k,m}) \\ &\qquad\qquad m = 1, 2, \cdots, K \end{aligned} \tag{17}$$

where $S_{k,m}$ denotes the measurement covariance.

Substituting (16) into formula (17), the joint measurement likelihood function can be calculated as

$$\begin{aligned} &P_{lik}(z_k|M^i_k = m.z_{1:k-1}.M^i_{k-1}, r_{1:k}) \\ &= \begin{cases} N(z_{kj}|h(f(x_{k-1}, M^i_{k-1}), M_k = 1, r_k), S_{k,1}), & if\ M_k = 1 \\ N(z_{kj}|h(f(x_{k-1}, M^i_{k-1}), M_k = 2, r_k), S_{k,1}), & if\ M_k = 2 \\ \qquad\qquad\vdots \\ N(z_{kj}|h(f(x_{k-1}, M^i_{k-1}), M_k = K, r_k), S_{k,1}), & if\ M_k = K \end{cases} \\ &\quad s.t.\ \left\{x_{m,k}\right\} \in \wp_k \end{aligned} \tag{18}$$

where the set $r_k = \{r^1_k, r^2_k, \cdots, r^c_k\}$ which include c independent components denote the target motion features irrelevant to the observation z_k.

Thus, the importance function of model particle can be established recursively as

$$\begin{aligned} &\pi(M_k|z_{1:k}, M^i_{k-1}, r_{1:k}) \\ &\propto p_{lik}(z_k|M_k, z_{1:k-1}, r_{1:k}, M^i_{k-1})p(M_k|z_{1:k-1}, r_{1:k}, M^i_{k-1}) \\ &= p_{lik}(z_k|M_k, z_{1:k-1}, r_{1:k}, M^i_{k-1})p(M_k|M^i_{k-1}) \\ &\quad s.t.\ \left\{x_{m,k}\right\} \in \wp_k \end{aligned} \tag{19}$$

where the model particle M_k depends only on the previous model M^i_{k-1} due to the Markov chain. Such that, the importance weight can be formed as

$$\omega^i_k \propto \omega^i_{k-1}\frac{p(z_k|M^i_k, z_{1:k-1}, r_{1:k}, M^i_{k-1})p(M_k|M^i_{k-1})}{\pi(M_k|z_{1:k}, M^i_{k-1}, r_{1:k})} \qquad i = 1, \cdots, N \tag{20}$$

and can be normalized as

$$\omega^i_k = \omega^i_{k-1}\left[\sum\nolimits_i^N \omega^i_k\right]^{-1} \qquad i = 1, \cdots, N \tag{21}$$

Based on the deductions above, Table 1 summarized the MSIR method to estimate model set $\left\{M^i_k\right\}^N_{i=1}$.

TABLE 1. Model-set estimate by MSIR.

1.Model-set (re)initialization $\{M_1^i\}_{i=1}^{Ns} = 1$
2. Calculate the measurement likelihood using (18);
3. Draw new model particles $\{M_k^i\}_{i=1}^{Ns}, k = 2, \cdots, N$
4. Normalize the importance distributions and replace them using (21).
6. Resample

What is essential in the evolution of the algorithm 1 is the model particles and their associated importance weights.

B. MODEL-CONDITIONED STATE ESTIMATE

The objective of this subsection is to estimate the model-conditioned state. From the hypothesis 1) in Section II, with Bayes' rule, the full posterior PDF of model-conditioned target state $x_{m,k}$ can be derived as (22), as shown at the bottom of this page, where ε is a normalized constant.

Due to constraints, the initial prior PDF becomes a truncated form, $P_1(\cdot)$, ie.,

$$\begin{aligned} &p_1(x_{m,k}|z_k, x_{k-1}, M_{k-1}^i, r_{1:k}) \\ &\quad = p_0(x_{m,k}|x_{k-1}, M_{k-1}^i, z_{1:k-1}, r_{1:k}) p_g(x_{m,k}, r_k) \end{aligned} \tag{23}$$

where $p_g(x_{m,k}, r_k)$ denotes the indicator function defined in Equation (12). According to the results of (29) and (31) derived in the later subsection 1), when the measurement noise variance is low, the modified PDF $p_1(\cdot)$ can significantly reduce the covariance of the prior PDF $p_0(\cdot)$ and improve the state estimation performance.

Considering the influence of past and current observation on state estimate adaptively, the proposal distribution of model-conditioned state can be jointly constructed as

$$\begin{aligned} &\pi(x_{m,k}|z_{1:k}, x_{0:k-1}, M_{k-1}^i, r_{1:k}) \\ &\quad = \alpha_k p_1(x_{m,k}|z_k, M_{k-1}^i, x_{k-1}, r_{1:k}) \\ &\qquad + (1-\alpha_k) p_0(x_{m,k}|x_{k-1}, M_{k-1}^i, z_{k-1}) \end{aligned} \tag{24}$$

where parameter $\alpha_k \in [0, 1]$ maintains a freedom degree to meet Bayes' rule, and its definition can be found in the Section 2).

Correspondingly, the importance weight for sampled particle at time k can be updated as (25), as shown at the bottom of this page, where $x_{m,k}^i$ denotes the *ith* model-conditioned state particle at time k.

The update process above implies that all the sampled particles fall into the feasible area which satisfies the constrained condition with a non-zero weight.

1) APPROXIMATION OF $p_1(\cdot)$

Apparently, it is almost impossible to sample directly from the proposal distribution defined in (19). To address this problem, we approximate the prior PDF $p_0(\cdot)$ and the modified prior PDF $p_1(\cdot)$ as Gaussian distributions and fuse the filtered results to form the final approximation of the a posterior PDF. To this end, the target vector can be rewritten as $x_k = [a_k^T, b_k^T]^T$,where $a_k \in R^{n_a}$ and $b_k \in R^{n_b}$ denotes the position and velocity vector, respectively, and $n_x = n_a + n_b$. And the following assumptions are reasonable: AP1), The nonlinear measurement function $h_k(\cdot)$ can be locally linearized; AP2), The marginal prior $p_{m,k}(a_{m,k})$ of the position vector is constant over the region I_{ek}; and AP3), The truncated measurement noise has the same first two moments as the real noise, i.e., $E[e_k] = 0$ and $cov[e_k] = R_k$.

With AP1), the measurement function $h_k(\cdot)$ can be approximated as $a_{m,k} = \hat{\phi}(z_k)$ using a first-order Taylor series. We choose $\hat{\phi}(z_k) = \arg\max_{a_{m,k}} p(z|a_{m,k})$ because it is the most likely observable state according to the measurement. If AP1) holds, $h_k(a_{m,k})$ can be calculated by

$$h_k(a_{m,k}) \approx h(\hat{\phi}(z_k)) + \tilde{H}_k^{-1}(a_{m,k} - \hat{\phi}(z_k)) \tag{26}$$

where $\tilde{H}_k^{-1} = [\nabla_{a_k} h_k^T(a_k)]^T|_{a_k=\hat{\phi}(z_k)}$ is the Jacobian of $h_k(a_{m,k})$ evaluated at $\hat{\phi}(z_k)$.

$$\begin{aligned} p(x_{m,k}|z_{1:k}, r_{1:k}) &= \frac{p(z_k|x_{0:k}, z_{1:k}) p(x_k|x_{1:k-1}, z_{1:k-1}) p(x_{1:k-1}|z_{1:k-1})}{p(z_k|z_{1:k-1})} \\ &= \frac{p(z_k - h(a_k)) p_g(a_{m,k}, r_k) p(x_{m,k}|x_{1:k-1}, M_{k-1}^i, z_{1:k}, r_{1:k}) p_0(x_{m,k-1}|M_{k-1}^i, z_{1:k-1}, r_{1:k-1})}{p(z_k, r_k|M_{k-1}^i, z_{1:k-1}, r_{1:k-1})} \\ &\propto p(z_k|x_{m,k}, r_{1:k}) p_1(x_{m,k}|z_k, x_{k-1}, M_{k-1}^i, r_{1:k})/\varepsilon \\ &\quad s.t.\ \{x_{m,k}\} \in \wp_k \end{aligned} \tag{22}$$

$$\begin{aligned} \omega_k^i &= \frac{p(x_{m,k}^i|z_{1:k}, r_{1:k})}{\pi(x_{m,k}^i|z_{1:k}, x_{0:k-1}, M_{k-1}^i, r_{1:k})} \\ &= \frac{p(z_k|x_{m,k}^i, r_{1:k}) p_1(x_{m,k}^i|z_k, x_{k-1}, r_{1:k}) p(x_{k-1}^i|M_{k-1}^i, z_{1:k-1}, r_{1:k-1})}{\pi(x_{m,k}^i|x_{k-1}^i, z_{1:k-1}, r_{1:k}) \pi(x_{k-1}^i|z_{1:k-1}, M_{k-1}^i, r_{1:k-1})} \\ &\propto \omega_{k-1}^i \frac{p(z_k|x_{m,k}^i, r_{1:k}) p_1(x_{m,k}^i|z_k, x_{k-1}, r_{1:k})}{\pi(x_{m,k}^i|x_{k-1}^i, z_{1:k}, r_{1:k})} \\ &\propto \omega_{k-1}^i p(z_k|x_{k,m}^i, r_{1:k}) \end{aligned} \tag{25}$$

Integrating out variable b, with AP2) and AP3), the mean and covariance of the prior PDF $p_i(\cdot), i = 0, 1$ can be derived as

$$\mu_{a_{i,k}} = \int a p_i(a; z) da = \hat{\phi}(z_k) \tag{27}$$

$$\begin{aligned}\sum\nolimits_{a_{i,k}} &= \int (a_{i,k} - \mu_{i,a})(a_{i,k} - \mu_{i,k})^T p_{i,k}(a; z) da \\ &= \tilde{H}^{-1} R (\tilde{H}^{-1})^T\end{aligned} \tag{28}$$

Thus, the corresponding mean $\hat{x}_{i,m,k}$ and covariance matrix $p_{i,m,k}$ can be factorized as

$$\hat{x}_{i,m,k} = \begin{bmatrix} E(a_{i,m,k}) \\ E(b_{i,m,k}) \end{bmatrix} = \begin{bmatrix} \mu_{a_{i,m,k}} \\ \mu_{b_{i,m,k}} \end{bmatrix} \tag{29}$$

$$\begin{aligned} p_{i,m,k} &= \begin{bmatrix} \mathrm{cov}(a_{i,m,k}) & \mathrm{cov}(a_{i,m,k}, b_{i,m,k}) \\ \mathrm{cov}(a_{i,m,k}, b_{i,m,k}) & \mathrm{cov}(b_{i,m,k}) \end{bmatrix} \\ &= \begin{bmatrix} \sum_{a_{i,m,k}} & \sum_{ab_{i,m,k}} \\ \sum^T_{ab_{i,m,k}} & \sum_{b_{i,m,k}} \end{bmatrix} \end{aligned} \tag{30}$$

In this manner the semi-positive definite or negative covariance matrix caused by the truncated error can be avoided. And the definitions of $\mu_{a_{0,m,k}}$, $\mu_{b_{0,m,k}}$, $\sum_{a_{0,m,k}}$, $\sum_{b_{0,m,k}}$ and $\sum_{ab_{0,m,k}}$ of the prior PDF can be referenced as in literature [16]. Equivalently, the mean $\hat{x}_{1,m,k}$ and covariance $p_{1,m,k}$ of the modified prior PDF $p_1(\cdot)$ can be calculated by

$$\hat{x}_{1,m,k} = \begin{bmatrix} E(a_{1,m,k}) \\ E(b_{1,m,k}) \end{bmatrix} = \begin{bmatrix} \mu_{a_{1,m,k}} \\ \mu_{b_{1,m,k}} \end{bmatrix} \tag{31}$$

$$p_{1,m,k} = \begin{bmatrix} \sum_{a_{1,m,k}} & \sum_{ab_{1,m,k}} \\ \sum^T_{ab_{1,m,k}} & \sum_{b_{1,m,k}} \end{bmatrix} \tag{32}$$

where $\mu_{a_{1,m,k}}$ and $\sum_{a_{1,m,k}}$ denote the mean and covariance of the position vector $a_{1,m,k}$, respectively. The details of $\mu_{b_{1,m,k}}$, $\sum_{b_{1,m,k}}$, $\sum_{a_{1,m,k}b_{1,m,k}}$ can be found in the literature [18].

Now, we use an adaptive least square method to estimate the state mean $\mu_{a_{1,mk}}$. To achieve high tracking accuracy, the auxiliary variables (actual target speed $\mathbf{v}$, time interval T, and heading angle θ) is incorporated to attain the maximum likelihood position $\hat{\phi}(z_k)$ defined as

$$\hat{\phi}(z_k) = \mu_{a_{k,0}} + K_k(\tilde{a}(z_k) - \tilde{H}_k^{-1}\mu_{a_{k,0}}) \tag{33}$$

$$K_k = (T^2 \cdot v^2 \cdot \sigma_v^2(k))/(\lambda \cdot \sigma_m^2(k) + T^2 \cdot v^2 \cdot \sigma_v^2(k)) \tag{34}$$

where $\tilde{a}(z_k) = (\hat{x}_T, \hat{y}_T, \hat{z}_T)$ denotes the target estimate position vector,λ is a constant factor,$\sigma_m^2(k)$ denotes the variance of measurement noise, and $\sigma_v^2(k)$ denotes the innovation variance. $\hat{\phi}(z_k)$ is considered as the latest measurement, and then, the mean $\mu_{a_{m,k},1}$ and the covariance $\sum_{a_{m,k},1}$ can be approximated as

$$\mu_{a_{1,m,k}} = \hat{\phi}(z_k) \tag{35}$$

$$\Sigma_{a_{1,m,k}} = \tilde{H}_k^{-1} R_k (\tilde{H}_k^{-1})^T = diag[\sigma_{\hat{x}_T}, \sigma_{\hat{y}_T}, \sigma_{\hat{z}_T}] \tag{36}$$

where $(\sigma_{\hat{x}_T}, \sigma_{\hat{y}_T}, \sigma_{\hat{z}_T})$ denotes the STD of the target state in the x, y, z coordinates.

Finally, the modified prior PDF $p_{1,m,k}(\cdot)$ can be approximated as a Gaussian distribution with mean $\hat{x}_{p_{1,m,k}}$ and variance $p_{p_{1,m,k}}$, i.e.,

$$p_{1,m,k}(x_{m,k}|z_k, M^i_{k-1}, r_k) \approx N(\hat{x}_{p_{1,m,k}}, P_{p_{1,m,k}}) \tag{37}$$

2) FUSION OF THE STATE ESTIMATE

Now, the final problem to be solved is how to decide the coefficient α_k, which can reflect the time-varying aspect for a Markov dynamic system. When the target measurement z_k is relatively more accurate, the estimation based on the modified prior PDF $p_{1,m,k}(\cdot)$ is more credible, and α_k tends to 1, vice versa. The parameter be calculated by (38) and (39)

$$\mu_i(\hat{x}_{i,m,k}) = \frac{1}{\sqrt{|p_{i,m,k}|}} \cdot \exp\left(-\frac{(z_k - h_k(\hat{x}_{i,m,k}))^2}{2}\right) \quad i = 0, 1 \tag{38}$$

$$\alpha_k = \frac{\mu_1(\hat{x}_{1,m,k})}{\mu_0(\hat{x}_{0,m,k}) + \mu_1(\hat{x}_{1,m,k})} \tag{39}$$

where $\hat{x}_{i,m,k}, i = 0, 1$ is the mean of prior and modified prior PDF.

Based on the deductions above, the mean $\hat{x}_{m,k}$ and covariance $p_{m,k}$ of the final posterior PDF $p(x_{m,k}|z_{1:k}, r_{1:k})$ can be approximated jointly as

$$\hat{x}_{m,k|k} = \alpha_k \hat{x}_{1,m,k|k} + (1 - \alpha_k)\alpha_k \hat{x}_{0,m,k|k} \tag{40}$$

$$\begin{aligned} p_{m,k|k} &= \alpha_k[p_{1,m,k|k} + (\hat{x}_{1,m,k|k} - \hat{x}_{m,k|k})(\hat{x}_{1,m,k|k} - \hat{x}_{m,k|k})^T] \\ &\quad + (1 - \alpha_k)[p_{0,m,k|k} + (\hat{x}_{0,m,k|k} - \hat{x}_{m,k|k}) \\ &\quad \times (\hat{x}_{0,m,k|k} - \hat{x}_{m,k|k})^T] \end{aligned} \tag{41}$$

In such a manner, the proposed CMMPF method can use the past and current observation adaptively to improve the target state estimation accuracy. Then the final fusion of state estimation for all motion models are updated as

$$\hat{x}_{k|k} = \sum_{i=1}^{N} \omega^i_{m,k} \hat{x}_{m,k|k} \tag{42}$$

$$p_{k|k} = \sum_{i=1}^{N} \omega^i_{m,k} \left[p^i_{m,k} + (\hat{x}_{m,k} - \hat{x}^i_{m,k})(\hat{x}_{m,k} - \hat{x}^i_{m,k})^T\right] \tag{43}$$

where $\omega^i_{m,k}$ denotes the associated weight of the *ith* motion model at time k which can be found in Equation(20). For the next iteration step at time $k + 1$, the filtered outputs $(\hat{x}_{k|k}, \hat{p}_{k|k})$ and the current measurement z_{k+1} are taken as the input variables for the motion model estimation, allowing the state constraints and the latest observation into the prediction step, and enhance the accuracy of the model set estimation.

C. SUMMARY AND DISCUSSION

To summarize, the CMMPF algorithm proceeds as follows in table 2.

Taking advantage of the state bounds and constraints in the update process can yield more accurate tracking performance.

1) Unlike the Taylor series estimation (TSE)-based linearization methods such as EKF, UKF which have the major

TABLE 2. Constrained Multiple Model Particle Filtering.

1. Initialization

The initial position vector x_0 and covariance p_0 are given by the measurement, and the process and measurement noise are white noise sequences with zero mean and the known covariance. Set the initial motion model m equals to 1, i.e., $\{M_1^i\}_{i=1}^N = 1$.

2. $k = 1$,Compute the propagated quantities x_k and z_k using equation (1) and (2) for each particle;

3. Estimate the model-set from algorithm 1.

4. State update based on the prior PDF $p_{0,m,k}(\cdot)$.

a. Draw N_s particles from the prior PDF $p_{0,m,k}(\cdot)$ and denote them as $\{x_{0,k,m}\}_{j=1}^{N_s}$.

b. Calculate associated weights using $\omega_{p_{0,k}}^i = p(z_k \mid x_{p_{0,k}}^i)$.

c. Normalize the importance weights $\omega_{p_{0,k}}^i$ to $\omega_{p_{0,k}}^i = \omega_{p_{0,k}}^i / \sum_{i=1}^{Ns} \omega_{p_{0,k}}^i$.

d. Estimate the mean $\hat{x}_{0,k}$ and covariance $\hat{p}_{0,k}$ based on $p_{0,m,k}(\cdot)$ using (44) and (45).

$$\hat{x}_{0,k|k} = \sum_{i=1}^{Ns} \omega_{p_{0,k}}^i x_{p_{0,k}}^i \tag{44}$$

$$\hat{p}_{0,k|k} = \sum_{i=1}^{Ns} \omega_{p_{0,k}}^i (x_{p_{0,k}}^i - \hat{x}_{p_{0,k}}^i)(x_{p_{0,k}}^i - \hat{x}_{p_{0,k}}^i)^T \tag{45}$$

5. State update based on the prior PDF $p_{1,m,k}(\cdot)$.

a. Calculate the mean $\hat{x}_{1,k}$ and covariance $\hat{p}_{1,k}$ of the modified prior PDF $p_{1,m,k}(\cdot)$ using (31) and (32).

b. Draw N_s particles from the prior PDF $p_{1,m,k}(\cdot)$ and denote them as $\{x_{1,k,m}\}_{j=1}^{N_s}$.

c. Calculate associated weights using $\omega_{p_{1,k}}^i = p(z_k \mid x_{p_{1,k}}^i)$.

d. Normalize the importance weights $\omega_{p_{1,k}}^i$ to $\omega_{p_{1,k}}^i = \omega_{p_{1,k}}^i / \sum_{i=1}^{Ns} \omega_{p_{1,k}}^i$.

e. Calculate the mean $\hat{x}_{u_{p_{1,k}}}$ and covariance $p_{u_{p_{1,k}}}$ based on $p_{1,m,k}(\cdot)$ using (46) and (47).

$$\hat{x}_{1,k|k} = \sum_{i=1}^{Ns} \omega_{p_{1,k}}^i x_{p_{1,k}}^i \tag{46}$$

$$\hat{p}_{1,k|k} = \sum_{i=1}^{Ns} \omega_{p_{1,k}}^i (x_{p_{1,k}}^i - \hat{x}_{p_{1,k}}^i)(x_{p_{1,k}}^i - \hat{x}_{p_{1,k}}^i)^T \tag{47}$$

6. Calculate the parameter α_k using (38) and (39).

7. Jointly update the posterior PDF using (40) and (41).

8. Update the final state estimation using (42) and (43).

Move to the next time step and repeat the cycle steps from 3 to the end.

limitation of local linearization of the nonlinear model and Gaussian noise model, CMMPF uses sequential Monte Carlo (SMC) method, also known as particle filters (PFs) to approximate multi-dimensional integration by a finite of set samples, the technique can deal with nonlinear and non-Gaussian distribution model effectively.

2) Unlike the conventional IMM-based filters which ignore the latest measurement in the first interacting stage, CMMPF estimate the model-set using MSIR method which introduces the current measurement information into the proposal distribution, enhancing the estimation accuracy other than using of only the historical measurement information.

3) Like the conventional auxiliary particle filter (APF), for model-conditioned state filtering CMMPF uses target spatio-temporal features as the auxiliary variables to guarantee the diversity and accuracy of samples. Furthermore, CMMPF takes account into the state bounds and constraints during the update proceeding, the optimization yields modified prior density that can explicitly account for bounds on state.

4) Additionally, to consider the influence of past and current measurement on the estimate, the hybrid importance distribution is established constants of prior and modified prior PDF.

IV. EXPERIMENT RESULTS

To evaluate the tracking performance of CMMPF for bearings-only maneuvering target tracking problem, a set of 100MC simulation are carried out in two simulation scenarios: (a) uniform and time-invariant sampling scenario. (b) non-uniform and time-varying sparse sampling scenario. The two passive sensors are located at the y-coordinate of the coordinate system as (0,5km,0) and (0, $-5km$,0), respectively. The constant turn rate is set to $w = 3°/s$. The model m_k in effect at $(k-1, k]$ is modeled by a time homogeneous 3-state first-order Markov chain with known transition probability matrix Π [7], whose elements are given as

$$\Pi = \begin{bmatrix} 0.98 & 0.01 & 0.01 \\ 0.1 & 0.8 & 0.1 \\ 0.1 & 0.1 & 0.8 \end{bmatrix} \tag{48}$$

Before the MC proceeding, we give a description of the three performance metrics that will be used in the analysis: (1) root mean square(RMS) position error, (2) efficiency η, (3) root time-averaged mean square (RATMS) error [7]. To define each of the above performance metrics, let (x_k^i, y_k^i, z_k^i) and $(\hat{x}_k^i, \hat{y}_k^i, \hat{z}_k^i)$ denote the true and estimated target positions at time k at the *ith* MC run, respectively. Suppose M of each MC runs are carried out. Then, the RMS position error at time k can be computed as

$$RMS_k = \sqrt{\frac{1}{M}\sum_{i=1}^{M} (\hat{x}_k^i - x_k^i)^2 + (\hat{y}_k^i - y_k^i)^2 + (\hat{z}_k^i - z_k^i)^2} \tag{49}$$

The Cramer-Rao lower bound can be used to give us a theoretical optimal bound on the expected errors between the estimated quantities and the true values from the known statistical properties of the measurement errors [5], which can be defined as

$$P = (H^T R^{-1} H)^{-1} \tag{50}$$

where H is Jacobian matrix. For the observation function (8), H can be calculated as (51), as shown at the bottom of the next page, where

$$(l_{j,k})^2 = (x_{j,k} - x_{s_j})^2 + (y_{j,k} - y_{s_j})^2 \tag{52}$$

$$(r_{j,k})^2 = (x_{j,k} - x_{s_j,k})^2 + (y_{j,k} - y_{s_j,k})^2 + (z_{j,k} - z_{s_j,k})^2 \tag{53}$$

where $j = 1, 2$ denotes the *jth* passive sensor.

The second metric stated above is the corresponding efficiency parameter for the matrix (9) defined as

$$\eta_k = \frac{CRLB(RMS_k)}{RMS_k} \times 100\% \tag{54}$$

which indicates "closeness" to CRLB. Thus, $\eta_k = 100\%$ implies an efficient estimation that achieve the CRLB exactly. For a particular scenario and parameters, like scenario A in this paper, the overall performance of a filter is evaluated using the third metric which is the RTAMS error. This is defined as

$$RTAMS = \sqrt{\frac{1}{(t_{\max}-l)M}\sum_{k=l+1}^{t_{\max}}\sum_{i=1}^{M}(\hat{x}_k^i-x_k^i)^2+(\hat{y}_k^i-y_k^i)^2+(\hat{z}_k^i-z_k^i)^2} \tag{55}$$

where $t_{\max}$ is the total number of observations (or time epochs) and l is a time index after which the averaging is carried out. Typically l is chosen to coincide with the end of the target maneuver.

A. UNIFORM AND TIME-INVARIANT SAMPLING SCENARIO

In this subsection a uniform and time-invariant sampling scenario is designed. A thorough and realistic performance comparison is carried out among the IMMEKF, IMMUKF, JMS-PF, MMPF and CMMPF trackers, including three aspects: process noise, measurement noise and sampling interval time. Fig. 1 shows the true simulated target trajectory. The real initial position of the target is ($2km$, $8km$, $1km$), and the initial velocity is ($0.19km/s$, $0.23km/s$, $0.00km/s$) and held invariant throughout the journey where the target makes two turns with rectilinear segments connecting them. The initial prior PDF of state is assumed to be $x_0 \sim N(\hat{x}_{0|0}, \hat{P}_{0|0})$, where

$$\begin{aligned}\hat{x}_{0|0} &= [2.1km \quad 0.12kms^{-1} \quad 7.95km \\ &\quad 0.23kms^{-1} \quad 0.95km \quad 0kms^{-1}] \\ \hat{P}_{0|0} &= diag[0.144km^2 \quad 0.02^2km^2s^{-2} \quad 0.144km^2 \\ &\quad 0.02^2km^2s^{-2} \quad 0 \quad 0]^T\end{aligned}$$

The trajectory segments are set as follows.

First Segment: Rectilinear flight until the plane is at ($4.85km$,$12.94km$,$1km$) from $t = 1s$ to $t = 25s$.

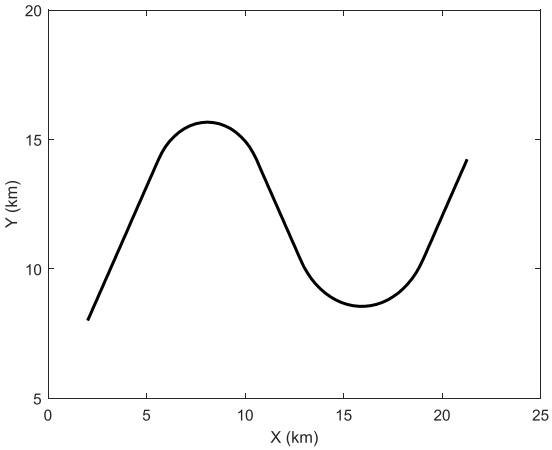

FIGURE 1. Simulated trajectory.

Second Segment: Circular maneuver mode with correct turn rate $5°/s$ until the plane is at ($10.56km$,$14.24km$, $1km$) from $t = 26s$ to $t = 45s$.

Third Segment: Rectilinear flight until the plane is at ($12.81km$,$10.34km$,$1km$), from $t = 46s$ to $t = 60s$.

Forth Segment: Circular maneuver mode with opposite turn rate $4°/s$ until the plane is at ($19.01km$, $10.34km$, $1km$) from $t = 61s$ to $t = 85s$.

Fifth Segment: Rectilinear flight until the plane is at ($21.26km$, $14.24km$, $1km$), from $t = 86s$ to $t = 100s$.

For PF-based filters, the number of particles was set as $N = 100$ to match the computational time, as preliminary runs indicate that policy refinement provides little improvement for the parameterization [22].

(1) Effect of process noise

We now investigate and compare the tracking performance of the filters with different process noise, when the observation noise is small, i.e., high signal-to-noise ratio. To do so, we fix the observation noise STD to be $1.5mrad/s$ and simulate three sets of process noise with STD as $0.005km/s^2$, $0.01km/s^2$ and $0.04km/s^2$, respectively. The interval time $T = 1s$. The RMS position error curves, against the theoretical bounds, are shown in Fig. 2. The probability of CV model switching being in effect is reported in Fig. 3. Table 3, 4 and 5 summarized the data in detail, including the mean and variance of RMSE, η, RTAMS and improvement. Note that the column "improvement" refers to the percentage

$$H(k+1) = \left.\frac{\partial h}{\partial X}\right|_{X=\hat{X}(k+1|k)} = \begin{bmatrix} -\frac{y_{j,k}-y_{s_j}}{(l_{j,k})^2} & 0 & -\frac{x_{j,k}-x_{s_j}}{(l_{j,k})^2} & 0 & 0 & 0 \\ -\frac{(x_{j,k}-x_{s_j})(z_{j,k}-z_{s_j})}{(r_{j,k})^2\sqrt{(l_{j,k})^2}} & 0 & -\frac{(y_{j,k}-y_{s_j})(z_{j,k}-z_{s_j})}{(r_k^{j_k})^2\sqrt{(l_{j,k})^2}} & 0 & \frac{\sqrt{(l_{j,k})^2}}{(r_{j,k})^2} & 0 \end{bmatrix} \quad j = 1, 2 \tag{51}$$

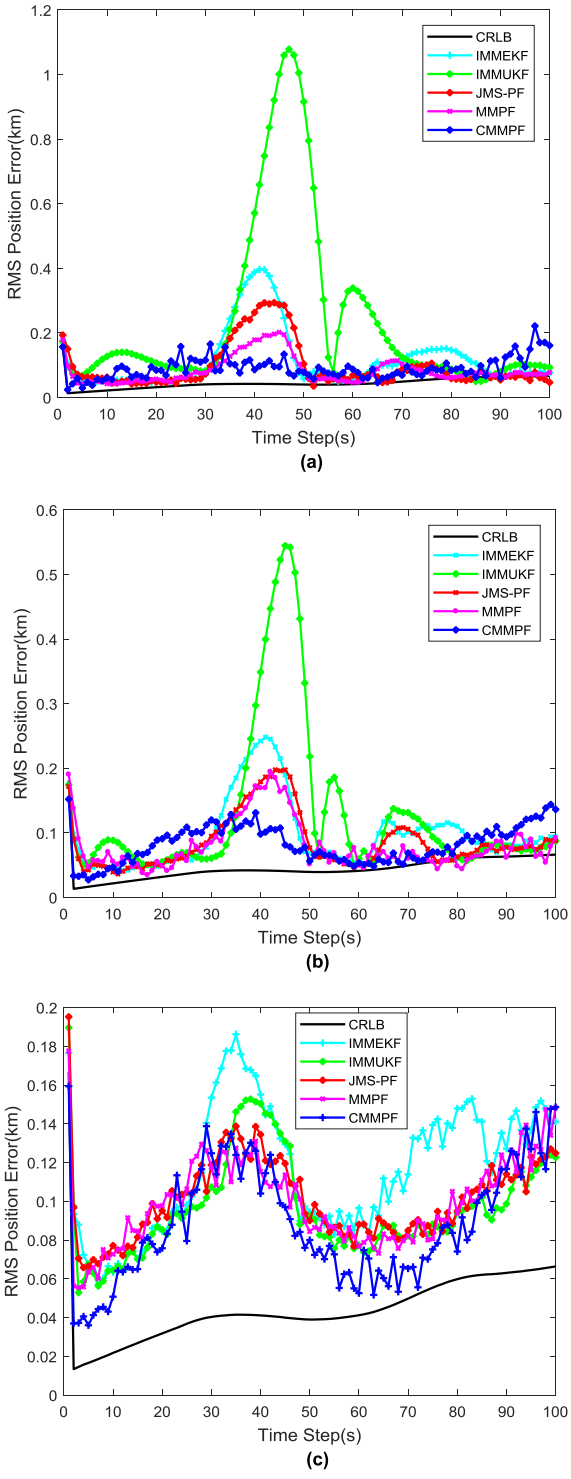

FIGURE 2. RMS position error versus time for a maneuvering target scenario with different process noise (a) $\sigma_v = 0.005km/s^2$. (b) $\sigma_v = 0.01km/s^2$. (c) $\sigma_v = 0.04km/s^2$.

improvement in RTAMS error compared with a chosen baseline filter with the worst filtering performance [7].

Results from Fig. 2 (a) and table 3 show that, (1) In the first smooth CV motion stage from $k = 1s$ to $k = 25s$, the overall RMS position errors of IMM-based KF-type filters

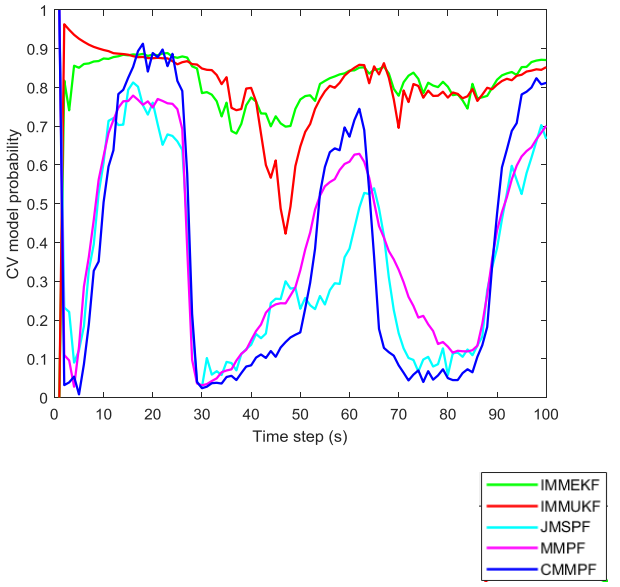

FIGURE 3. CV model switching probability $\sigma_v = 0.04km/s^2$.

TABLE 3. Performance comparison $\sigma_v = 0.005km/s^2$

Algorithm/ CRLB	RMSE mean(km)	RMSE variance(km^2)	η	RTAMS (km)	Improvement (%)
IMMEKF	0.113	0.007	38	0.405	0
IMMUKF	0.232	0.006	16	0.378	7
MMPF	0.096	0.002	45	0.329	19
JMS-PF	0.097	0.005	44	0.346	15
CMMPF	0.084	0.001	51	0.322	20
CRLB	0.043	------	100	0.160	60

are even smaller than PF-based filters for the smoothing and high signal-to-noise ratio segments. (2)When the target maneuvering occurs at time $k = 26s$, CMMPF algorithm presents a slight bubble in the RMSE curve correspondingly, while the other four algorithms show a relative larger bubble at $k = 30s$ due to a time delay. (3) After the target maneuver, CMMPF shows the smallest error during the maneuvering onset from $k = 26s$ to $k = 45s$, which is closest to the CRLB curve, while IMMUKF presents the highest peak error. The "closeness" to CRLB curve arranged from small to large for other filters is MMPF, JMS-PF and IMMEKF. The main reason for this is that, the target maneuvering has resulted in an observable geometry at that instant and a larger size of innovation covariance correspondingly, but the KF-type algorithms cannot update the gain and the covariance in time. While MMPF and CMMPF shows a superior performance. As can be seen from table 3, CMMPF has the smallest size of RTAMS, with the highest improvement 20% over the baseline filter IMMUKF. The JMS-PF on the other hand is worse than MMPF and CMMPF but better than IMMEKF/IMMUKF, as it uses an EKF to compute the mode history probability, due to the linearized approximation, even if the number of particles for JMS-PF is increased, its performance cannot reach that of MMPF/CMMPF.

Both the qualitative RMSE curves in Fig. 2 (b), (c) and the quantitative statistics in table 4, 5 indicate that, with the process noise increasing, the overall error gaps between the

TABLE 4. Performance comparison $\sigma_v = 0.01km/s^2$.

Algorithm/ CRLB	RMSE mean(km)	RMSE variance(km^2)	η	RTAMS (km)	Improvement (%)
IMMEKF	0.095	0.002	45	0.375	0
IMMUKF	0.129	0.001	33	0.329	11
MMPF	0.083	0.002	50	0.329	30
JMS-PF	0.085	0.002	51	0.346	26
CMMPF	0.076	0.001	56	0.322	32
CRLB	0.043	------	100	0.160	36

TABLE 5. Performance comparison $\sigma_v = 0.04km/s^2$.

Algorithm/ CRLB	RMSE mean(km)	RMSE variance(km^2)	η	RTAMS (km)	Improvement (%)
IMMEKF	0.101	0.001	4	0.554	0
IMMUKF	0.081	0.001	51	0.409	26
MMPF	0.089	0.001	47	0.342	38
JMS-PF	0.085	0.002	51	0.403	27
CMMPF	0.076	0.001	57	0.287	48
CRLB	0.043	------	100	0.160	71

algorithms is becoming narrower, all filters exhibit a decline tendency in the uniform motion period but a better tracking performance in the maneuvering period.

Fig. 3 shows the CV model switching curves with a process noise STD $0.04km/s^2$. For IMMEKF, the motion model hardly switches along with the target maneuvering, and the overall tracking results show a trend that deviates from the true orbit, this is consistent with the parameters listed in table 5 with the lowest η and largest RTAMS. IMMUKF also shows worse performance than MMPF and CMMPF obviously. The major reasons for this are (1) the basic premise of the EKF is that the errors are ''small'' enough so that a first-order expansion of the nonlinear model can sufficiently describes the errors at all times [5], like UKF, both filters assume that the posterior PDF is Gaussian, i.e., the PDF is unimodal. When dealing with nonlinear systems this may no longer be true, even with Gaussian inputs into the nonlinear model. While the CMMPF can capture the target maneuvering behavior well for the same settings because it utilizes both the state constraints and target motion features in the state updating process effectively, after the target maneuvering, the RTAMS improvement over the baseline filter IMMEFK is 48%, nearest to the CRLB whose improvement is 71%.

TABLE 6. Comparison of the computation time.

Algorithm	IMMEKF	IMMUKF	JMS-PF	MMPF	CMMPF
Time(s)	0.04	0.07	13.96	38.7	47.5

Finally, table 6 summarized the average computation time needed for 100 MC runs of different algorithms in the second case. Obviously, the PF-based multiple model methods have an expensive computation load mainly because of the increased Monte Carlo calculations in the state nonlinear filtering process.

(2) Effect of measurement noise

Here we investigate the tracking performance for bearings-only maneuvering target tracking when the observation noise

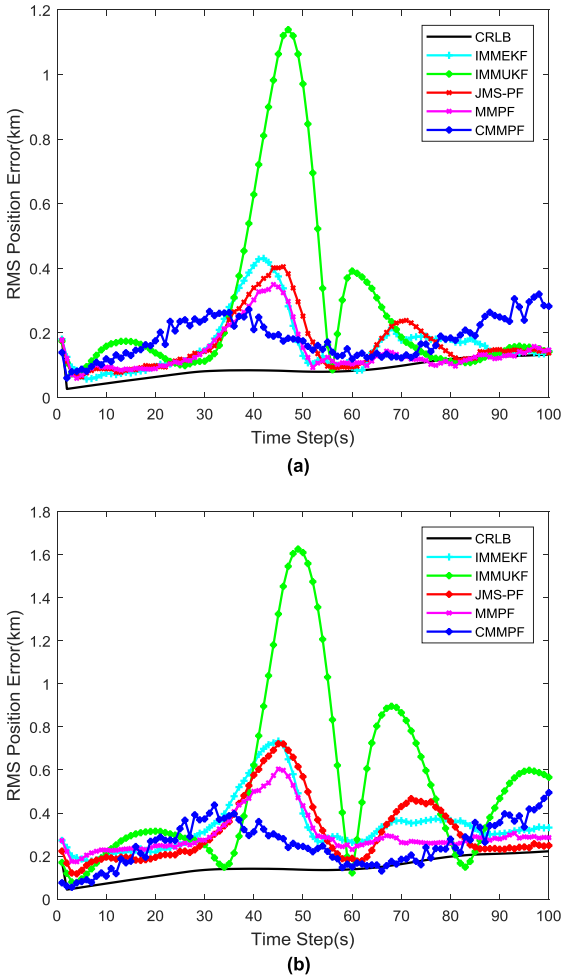

FIGURE 4. The RMS position error versus time under different measurement noise. (a) $\sigma_e = 3mrad/s$. (b) $\sigma_e = 5mrad/s$.

is larger, i.e., signal-to-noise ratio is lower. To do so, we fix the process noise STD to be $0.01km/s^2$ and select three sets of observation noise with STD as $1.5mrad/s$, $3mrad/s$, and $5mrad/s$, respectively. The interval time $T = 1s$. The qualitative RMS position error curves, against the theoretical bounds, are shown in Fig. 2(b) and Fig. 4. Table 7 and 8 summarized the data statistics in detail. Noting that the performance comparison with measurement noise STD $1.5mrad/s$ is the same as the second one in case (1), with the same results in Fig. 2(b) and table 4, which is not repeatedly given here.

Simulation results show that, the parameter values, both RMSE and RTAMS, of all filters exhibit an increment as the measurement noise increases. Like the analysis in case (1), CMMPF indicates advantages over the other existing filters with respect to accuracy, efficiency and robustness.

It is worth noting that in the above simulations, the performance of MMPF is comparable to that of the CMMPF due to the small process noise used in the uniform sampling simulations. However, for bearings-only maneuvering target tracking problem with larger interval time and moderate

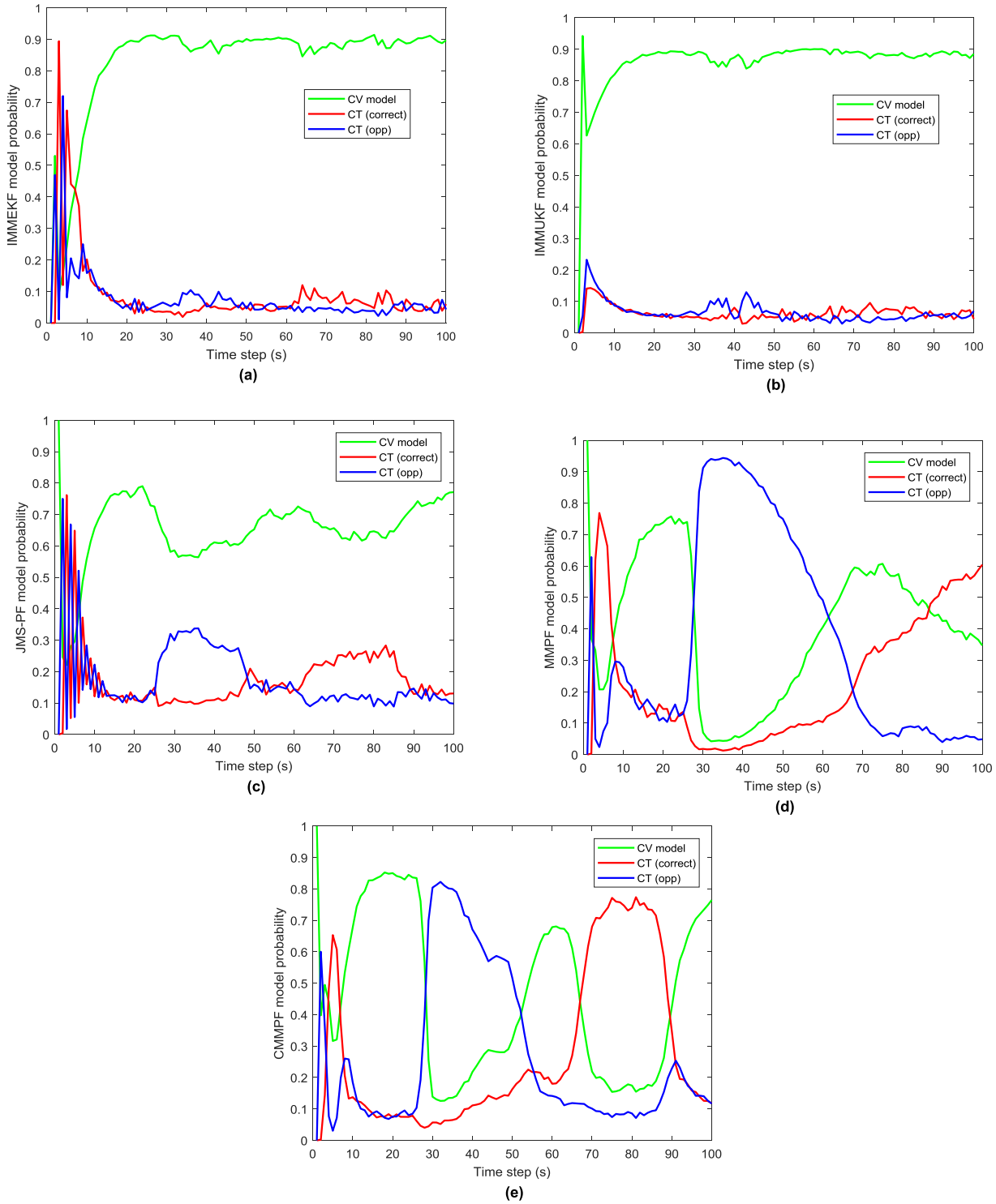

FIGURE 5. Model switching probability with sampling time T=3s (a) IMMEKF. (b) IMMUKF. (c) JMS-PF. (d) MMPF. (e) CMMPF.

to high process noise, the CMMPF is likely to outperform the MMPF.

(3) Effect of sampling interval time

Now, we will investigate the effect of sampling interval time for the bearings-only maneuvering target tracking in the uniform sampling and time-invariant scenario. The interval time is set to relatively larger as $T = 3s$, the STD of process and measurement noise is $0.01km/s^2$ and $1.5mrad/s$, respectively. The motion model set switching probability curves for the five multiple model based filters are shown in Fig. 5.

TABLE 7. Performance comparison $\sigma_e = 3mrad/s$.

Algorithm/ CRLB	RMSE mean(km)	RMSE variance(km^2)	η	RTAMS (km)	Improvement (%)
IMMEKF	0.162	0.003	53	0.965	10
IMMUKF	0.279	0.002	31	0.866	0
MMPF	0.214	0.002	40	0.609	37
JMS-PF	0.218	0.002	40	0.631	35
CMMPF	0.146	0.001	59	0.579	40
CRLB	0.086	------	100	0.189	80

TABLE 8. Performance comparison $\sigma_e = 5mrad/s$.

Algorithm/ CRLB	RMSE mean(km)	RMSE variance(km^2)	η	RTAMS (km)	Improvement (%)
IMMEKF	0.532	0.163	27	0.945	36
IMMUKF	0.945	0.034	15	1.489	0
MMPF	0.354	0.009	41	0.904	39
JMS-PF	0.265	0.023	54	1.063	28
CMMPF	0.201	0.010	72	0.818	45
CRLB	0.144	------	100	0.328	78

Obviously, although there is a slight bump in the model probability for the correct turn model, the IMM-based algorithms are unable to switch from the first CV model to the other CT models. That is to say, they failed to capture the target maneuvering behavior for the sparse observation, mainly because of ignoring the latest observation information in the interacting stage. JMS-PF shows a better performance than IMMEKF and IMMUKF, but worse than MMPF and CMMF. For the same scene, meanwhile, CMMPF indicates a better ability to capture the target maneuvering behavior, because it estimates model-set with series of boundary optimization.

In summary, simulation results in this subsection indicate that CMMPF algorithm is the best one among the suboptimal algorithms in comparison with respect to RMS position error, efficiency η and RTAMS.

B. NON-UNIFORM TIME-VARYING AND SPARSE SAMPLING SCENARIO

In this subsection, we will investigate a real aperiodic sparse sampling aircraft tracking scenario, including 40 aperiodic sampling points, and the target flight time is $107s$. The sampling interval T is time-varying and can be defined as

$$T = t(k+1) - t(k) \tag{56}$$

where $t(k+1)$ and $t(k)$ denotes the sampling time at time $k+1$ and k, respectively. As the IMMEKF, IMMUKF and JMS-PF trackers show a divergence when the target is missed from measurement at $k = 25s$ due to an abrupt larger interval time, the track loss rates are high to 38%. Such that, we compare and analysis filtering performance of the ATPF, MMPF and CMMPF. The initial state prior PDF is given as $x_0 \sim N(\hat{x}_{0|0}, \hat{P}_{0|0})$, where

$$x_{0|0} = [6.331km - 0.031kms^{-1} \quad 2.589km \quad 0.29kms^{-1} \quad 1.0km \quad 0kms^{-1}]^T$$
$$\hat{p}_{0|0} = diag[0.15^2km^2 \quad 0km^2s^{-2} \quad 0.15^2km^2 \quad 0km^2s^{-2} \quad 0.15^2km^2 \quad 0km^2s^{-2}]^T.$$

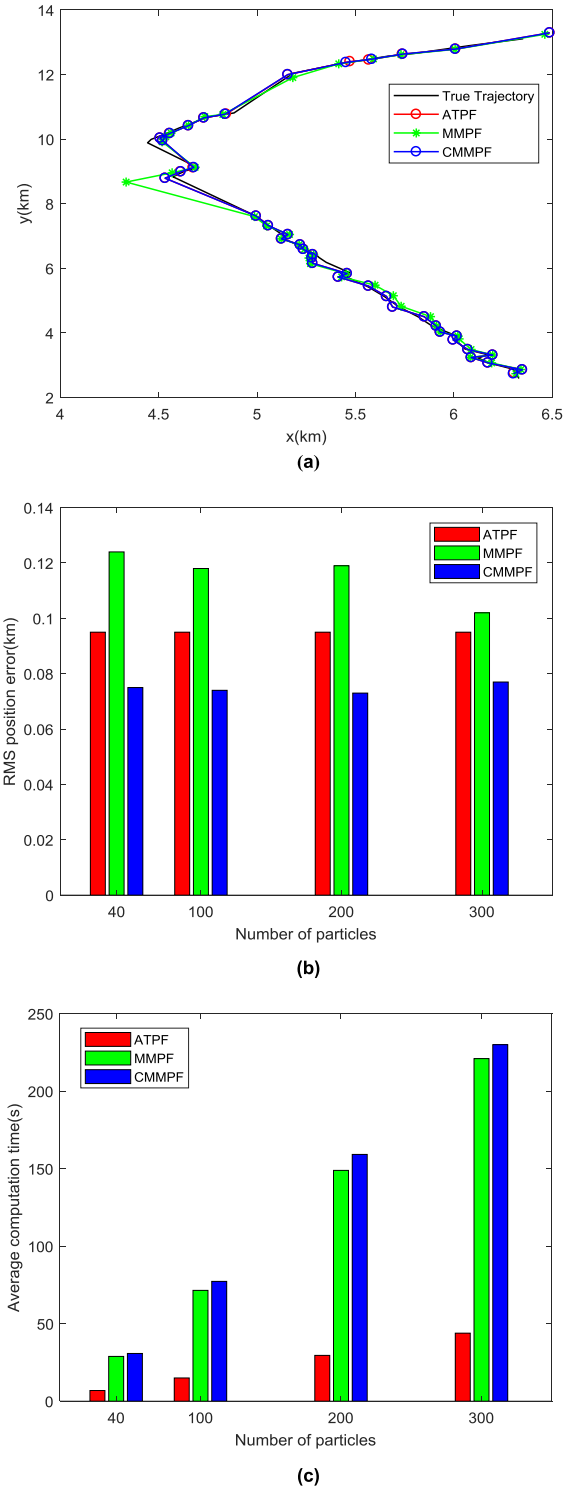

FIGURE 6. Filtering performance. (a) True and Estimated trajectories. (b) RMS position error with different number of particles. (c) Average computation time with different number of particles.

To evaluate the tracking performance under different numbers of particles, we set the number of particles as 40, 100, 200 and 300. The STD of process and measurement noise is $0.2km/s^2$ and $3mrad/s$, respectively. 100 MC runs are carried out.

The true and estimated trajectories are shown in Fig. 6 (a). Statistics of RMS position error and average execution time needed for 100 MC runs are shown in Fig. 6 (b) and (c), respectively.

Compared with ATPF and MMPF algorithm, the overall RMS position error of CMMPF decreases near 22.1% and 39.5%, respectively. The major reasons are that (i) CMMPF estimates the model-set in an optimal manner, takes advantage of the nonlinear soft state constraints in every step of the state update. (ii) CMMPF simultaneously incorporates the current measurement and spatio-temporal features as auxiliary variables into the proposal distribution for nonlinear state filtering. Thus it can deal with the motion model uncertainty effectively.

Additionally, since the tracking performance shows no significant improvement as the number of particle increases while the execution time increases much more. It is reasonable to reduce the number of particle to trade off the estimate accuracy and calculation load.

V. CONCLUSIONS

One of the major challenges for target tracking arises from the target motion uncertainty and observation nonlinearity, furthermore, the state constraint is another challenge should not be ignored. In this regard, we have proposed a novel and efficient constrained multiple model particle filter for bearings-only maneuvering target tracking, there are four distinguished features for the algorithm

1) To save the high-dimension calculation load and reduce the error covariance, CMMPF divides the dynamic state space into two sub-problems according to the Rao-Blackwellised theorem.
2) For model set estimate, the algorithm utilizes a MSIR method to restrict the samples into a feasible area consistent with the constraint boundary, and simulation model switching curves are consistent with the target maneuvering trajectory.
3) The approach shows merits for nonlinear non-Gaussian problem, because the estimator approximates the posterior distribution without necessary linearization or high order differential matrix.
4) For the model-conditioned state nonlinear filtering, the tracker approximates the truncated prior density by LS method, incorporates the latest measurement and target spatio-temporal features into the proposal distribution effectively, the diversity and accuracy of the sampled particles can be guaranteed.

Experiment results confirm that the proposed CMMPF algorithm has a distinguished advantage over the other filters in comparison in this paper when dealing with the bearings-only target maneuvering tracking problem, especially, in the aperiodic and sparse sampling environment. The main drawback of CMMPF is the calculation load, which is to be addressed in our future work. We will extend this algorithm to multi-target tracking in clutter environments and make corresponding improvements.

REFERENCES

[1] S. C. Nardone, A. G. Lindgren, and K. F. Gong, "Fundamental properties and performance of conventional bearings-only target motion analysis," *IEEE Trans. Autom. Control*, vol. AC-29, no. 9, pp. 775–787, Sep. 1984.
[2] T. L. Song, "Observability of target tracking with bearings-only measurements," *IEEE Trans. Aerosp. Electron. Syst.*, vol. 32, no. 4, pp. 1468–1472, Oct. 1996.
[3] M. Ye, B. D. O. Anderson, and C. Yu, "Bearing-only measurement self-localization, velocity consensus and formation control," *IEEE Trans. Aerosp. Electron. Syst.*, vol. 53, no. 2, pp. 575–586, Apr. 2017.
[4] X. R. Li and V. P. Jilkov, "Survey of maneuvering target tracking—Part I. Dynamic models," *IEEE Trans. Aerosp. Electron. Syst.*, vol. 39, no. 4, pp. 1333–1364, Oct. 2004.
[5] J. L. Crassidis and J. L. Junkins, *Optimal Estimation of Dynamic Systems*, 2nd ed. London, U.K.: Chapman & Hall, 2011, pp. 249–253.
[6] X. R. Li and Y. Bar-Shalom, "Design of an interacting multiple model algorithm for air traffic control tracking," *IEEE Trans. Control Syst. Technol.*, vol. 1, no. 3, pp. 186–194, Sep. 1993.
[7] M. S. Arulampalam, B. Ristic, N. Gordon, and T. Mansell, "Bearings-only tracking of manoeuvring targets using particle lters," *EURASIP J. Adv. Signal Process.*, vol. 15, pp. 1–15, 2004.
[8] H. Sheng, W. Zhao, and J. Wang, "Interacting multiple model tracking algorithm fusing input estimation and best linear unbiased estimation filter," *IET Radar Sonar Navigat.*, vol. 11, no. 1, pp. 70–77, 2017.
[9] X. R. Li and V. P. Jilkov, "A survey of maneuvering target tracking, part VIc: Approximate nonlinear density filtering in discrete time," *Proc. SPIE*, vol. 8393, p. 83930V, May 2012, doi: 10.1117/12.921508.
[10] R. van der Merwe, A. Doucet, N. de Freitas, and E. Wan, "The unscented particle filter," in *Proc. Int. Conf. Neural Inf. Process. Syst.*, vol. 13. Cambridge, MA, USA: MIT Press, 2000, pp. 563–569.
[11] S. Konatowski, P. Kaniewski, and J. Matuszewski, "Comparison of estimation accuracy of EKF, UKF and PF filters," *Annu. Navigat.*, vol. 23, no. 1, pp. 69–87, 2016.
[12] N. J. Gordon, D. J. Salmond, and A. F. M. Smith, "Novel approach to nonlinear/non-Gaussian Bayesian state estimation," *IEE Proc. F, Radar Signal Process.*, vol. 140, no. 2, pp. 107–113, Apr. 1993.
[13] A. Doucet and A. M. Johansen, "A tutorial on particle filtering and smoothing: Fifteen years later," in *The Oxford Handbook of Nonlinear Filtering*, D. Crisan and B. Rozovsky, Eds. London, U.K.: Oxford Univ. Press, 2011, pp. 30–32.
[14] F. Lindsten, P. Bunch, S. Särkkä, T. B. Schön, S. J. Godsill, "Rao-blackwellized particle smoothers for conditionally linear Gaussian models," *IEEE J. Sel. Topics Signal Process.*, vol. 10, no. 2, pp. 353–365, Mar. 2016.
[15] J. Liu, Z. Wang, and M. Xu, "A Kalman estimation based Rao-blackwellized particle filtering for radar tracking," *IEEE Access*, vol. 5, pp. 8162–8174, 2017.
[16] Á. F. Garcia-Fernandez, R. M. Morelande, and J. Grajal, "Truncated unscented Kalman filtering," *IEEE Trans. Signal Process.*, vol. 60, no. 7, pp. 3372–3386, Jul. 2012.
[17] N. Amor, N. Bouaynaya, R. Shterenberg, and S. Chebbi, "On the convergence of constrained particle filters," *IEEE Signal Process. Lett.*, vol. 24, no. 6, pp. 858–862, Jun. 2017.
[18] L.-Q. Li, W.-X. Xie, and Z.-X. Liu, "Auxiliary truncated particle filtering with least-square method for bearings-only maneuvering target tracking," *IEEE Trans. Aerosp. Electron. Syst.*, vol. 52, no. 5, pp. 2562–2567, Oct. 2017.
[19] L. Xu, X. R. Li, Y. Liang, and Z. Duan, "Constrained dynamic systems: Generalized modeling and state estimation," *IEEE Trans. Aerosp. Electron. Syst.*, vol. 53, no. 5, pp. 2594–2609, Oct. 2017.
[20] J. Heng, A. N. Bishop, G. Deligiannidis, and A. Doucet. (2017). "Controlled sequential Monte Carlo." [Online]. Available: https://arxiv.org/abs/1708.08396
[21] A. Doucet, N. J. Gordon, and V. Krishnamurthy, "Particle filters for state estimation of jump Markov linear systems," *IEEE Trans. Signal Process.*, vol. 49, no. 3, pp. 613–624, Mar. 2001.
[22] V. Elvira, J. Míguez, and P. M. Djurić, "Adapting the number of particles in sequential Monte Carlo methods through an online scheme for convergence assessment," *IEEE Trans. Signal Process.*, vol. 65, no. 7, pp. 1781–1794, Apr. 2017.

HONGWEI ZHANG received the B.S. degree in electronic engineering from Zhengzhou University in 2006 and the M.S. degree from the South China University of Technology in 2013. She is currently pursuing the Ph.D. degree with the College of Information Engineering, Shenzhen University.

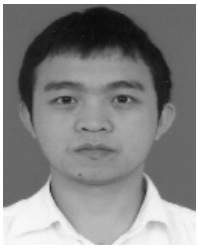

LIANGQUN LI received the B.S. degree in electronic engineering, the M.S. degree in signal and information processing, and the Ph.D. degree in pattern recognition and intelligent system from Xidian University, Xi'an, China, in 2002, 2005, and 2007, respectively. From 2007 to 2009, he was a Post-Doctoral Fellow with the ATR Key Laboratory, Shenzhen University, where he is currently a Professor. He has published one book and around 60 technical articles in refereed journals and international conferences in his research fields. His research interests include intelligent information processing, Fuzzy information processing, computer vision, multi object detection and tracking, radar multiple target tracking, and particle filtering.

WEIXIN XIE received the B.S. degree from Xidian University, Xi'an, in 1965. He joined the Faculty of Xidian University in 1965. From 1981 to 1983, he was a Visiting Scholar with the University of Pennsylvania, USA. In 1989, he was a Visiting Professor with the University of Pennsylvania. He is currently a Professor with Shenzhen University. His research interests include intelligent information processing and pattern recognition.